Grant Agreement No.: 604656

Project acronym: NanoSim

Project title: A Multiscale Simulation-Based Design Platform for Cost-Effective CO_2 Capture Processes using Nano-Structured Materials (NanoSim)

Funding scheme: Collaborative Project

Thematic Priority: NMP

THEME: [NMP.2013.1.4-1] Development of an integrated multi-scale modelling environment for nanomaterials and systems by design

Starting date of project: 1st of January, 2014

Duration: 48 months

WP N°	Del. N°	Title	Contributors	Version	Lead beneficiary	Nature	Dissemin. level	Delivery date from Annex I	Actual delivery date dd/mm/yyyy
5	5.3	Derivation of subgrid models for inter-particle species momentum transfers by collisions	INPT	1.0	INPT, NTNU	PU		01/01/2016	30/06/2016

1 Abstract

The report presents a model for taking into account the subgrid effect in the inter-particle momentum transfer by collisions.

The model is derived from an analysis highly resolved TFM numerical simulation. A correlation study is made in order to identify the relevant variables for the modelling. The effects of the mesh size and of the local solid volume fraction are split and modelled by two different functions. Finally the functions are determined by fitting.

In the present report only one case ($\alpha_p = \alpha_q = 3\%$ and $d_q = 2d_q = 150\mu m$) has been used. Then the model must be compared for volume fraction and particle-to-particle diameter ratio. Also, during the study it has been shown the strong effect of the filtering on the particle kinetic energy which controls the transfers by collisions.

2 Case studied

This report is devoted to the derivation of a subgrid model for the inter-particle momentum transfer. The model derivation is based on the analysis of the highly-resolved numerical simulations described in D5.1. The particles properties of the flow are given in Table 1 :

Gas		$\rho_g\,(kg/m^3)$	1,186
		$\mu_g\,(Pa.s)$	1,8 .10^{-5}
Particles 1		$d_q(\mu m)$	75
		$\rho_p(kg/m^3)$	1500
		α_p	3 %
Particles 2		$d_q\,(\mu m)$	150
		$\rho_q(kg/m^3)$	1500
		α_q	3%
	e_c		0,9

Table 1: Materials properties

3 Model derivation

3.1 Subgrid drag model in binary mixture

The budget and correlation analysis of the momentum balance equation show that drag force is affected by the mesh. The correlation analysis suggests that a subgrid gas-particle drift velocity exists and requires a modelling approach.

Following Igci et al. (2008), Parmentier et al. (2012), Ozel et al. (2013) the subgrid inter-particle drift velocity is defined as:

$$\tilde{\alpha}_p W_p^d = \alpha_p \widetilde{\left(W_p - W_g\right)} - \tilde{\alpha}_p \tilde{\alpha}_q \left(\widetilde{W}_p - \widetilde{W}_g \right)$$

Figure 1 shows the subgrid inter-particle drift flux, $\tilde{\alpha}_p W_p^d$, as a function of the resolved inter-particle drift flux, $\tilde{\alpha}_p (\widetilde{W}_p - \widetilde{W}_g)$ in the case of small particles and $\frac{\Delta}{\Delta_{ref}} = 6$. It appears that the two variables are correlated. It can be noticed that the same trend is observed for the large particles. Then a model for the subgrid drift flux can written in terms of the computed variables as:

$$\tilde{\alpha}_p W_p^d = g_p\left(\Delta^* , \tilde{\alpha}_p, \tilde{\alpha}_q\right) \tilde{\alpha}_p \left(\widetilde{W}_p - \widetilde{W}_g \right)$$

Where g_p is a function of the local solid volume fraction and of the mesh. This function can be computed as

$$g_p\left(\Delta^* , \tilde{\alpha}_p\right) = \frac{\overline{\langle \tilde{\alpha}_p W_p^d | \tilde{\alpha}_p \rangle}}{\overline{\langle \tilde{\alpha}_p \tilde{\alpha}_q (\widetilde{W}_p - \widetilde{W}_g) | \tilde{\alpha}_p \rangle}}$$

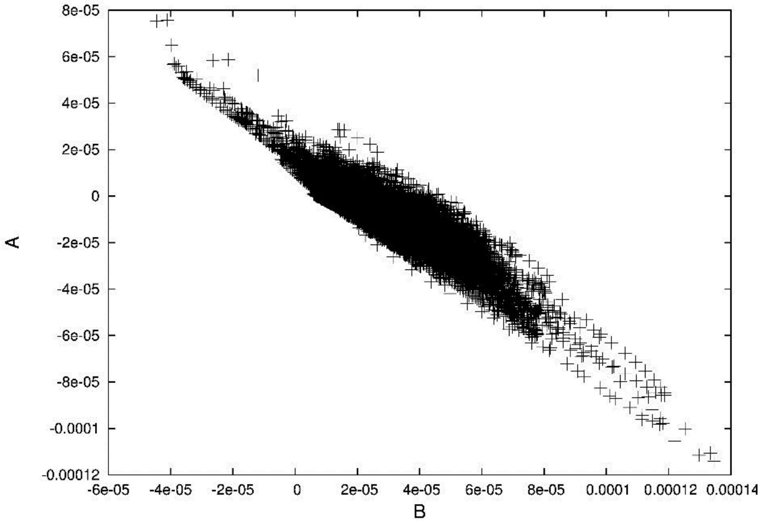

Figure 1: Scatter plot of the subgrid drift flux $A = \tilde{\alpha}_p W_p^d$ versus the resolved drift flux $B = \tilde{\alpha}_p \tilde{\alpha}_q (\widetilde{W}_p - \widetilde{W}_g)$ for $\frac{\Delta}{\Delta_{ref}} = 6$ for particles type p ($d_p = 75\ \mu m$)

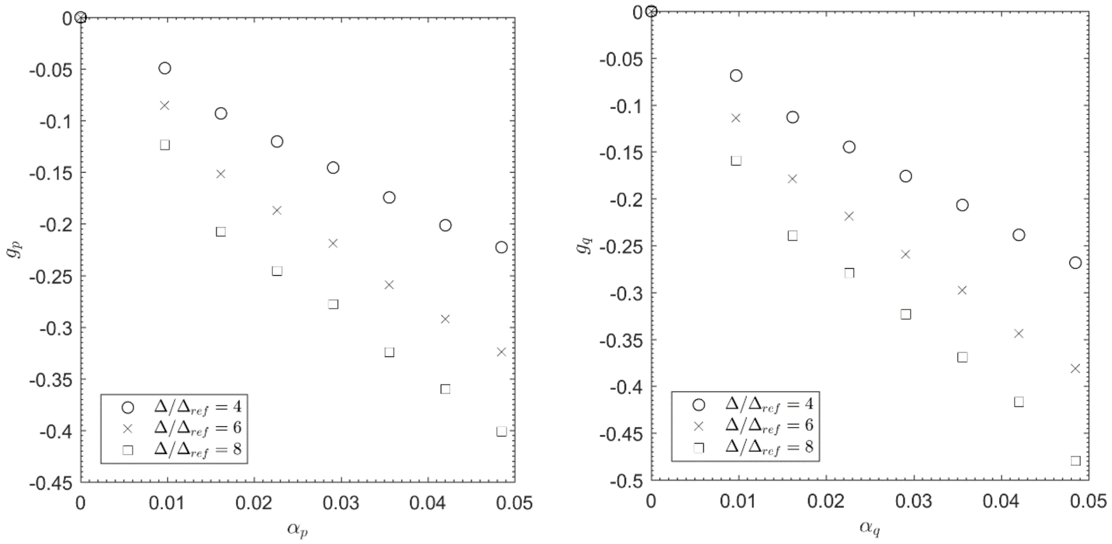

Figure 2: The function g for various filter widths

The calculated function $g_p(\Delta^*\ , \tilde{\alpha}_p)$ for different filter widths are shown by Figure 2. The shape of g is almost independent of the filter width, then we can decompose $g_p(\Delta^*, \tilde{\alpha}_p)$ as :

$$g_p(\Delta^*\ , \tilde{\alpha}_p) = f_p(\Delta^*\ ) h_p(\tilde{\alpha}_p)$$

The function g_p is not defined for $\alpha_p > 0.05$, indeed, there is not enough particles to define the function. The range of solid volume fraction will be $\alpha_p \in [0; 0{,}05]$. The function g_p is normalized by the area under the curve for each filter widths. A form of the function h_p is then proposed.

$$h_p(\tilde{\alpha}_p) = \left(1 + C_1 \left(\frac{\tilde{\alpha}_p}{\alpha_{max}}\right) \ + C_2 \left(\frac{\tilde{\alpha}_p}{\alpha_{max}}\right)^2 + C_3 \left(\frac{\tilde{\alpha}_p}{\alpha_{max}}\right)^3\right) \left(\frac{\tilde{\alpha}_p}{\alpha_{max}}\right)^{0.5}$$

with $C_1 = 5907$, $C_2 = 1{,}1089 \cdot 10^5$ and $C_3 = 6{,}851 \cdot 10^5$. This function verifies the condition, being equal to 0 when there is no particle.

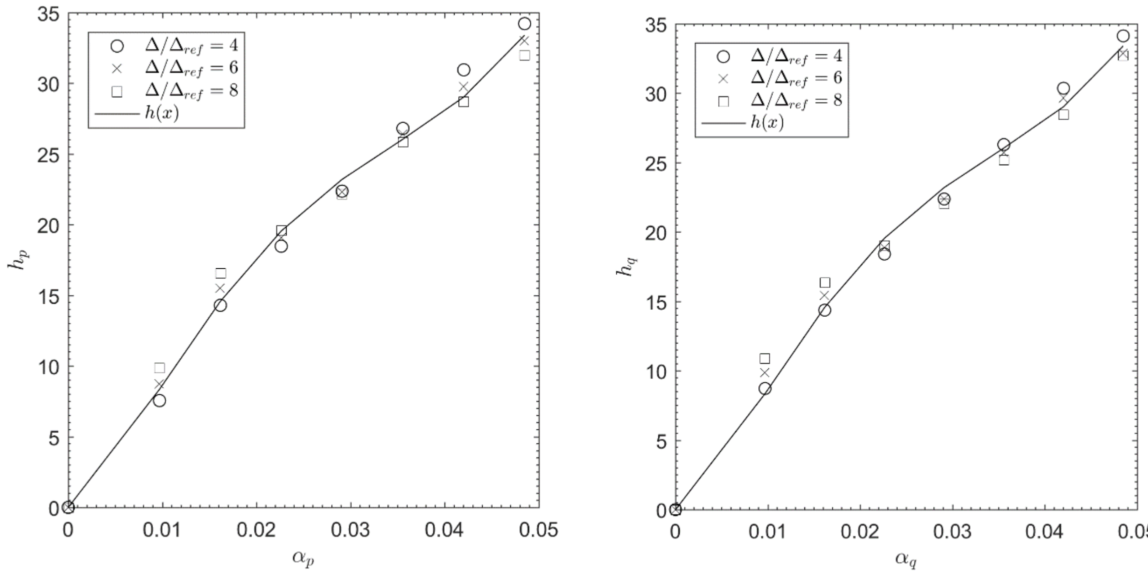

Figure 3: The measured function h_p for various filter widths (symbols) and the proposed correlation (solid lines)

Figure 3 shows that the same function can be sued for the small and the large particles.

The function $f_p(\Delta^*\ )$needs to be defined. The function f_p can be evaluated by:

$$f_p(\Delta^*\ ) = \frac{\overline{\langle \alpha_p W_p^d \rangle}}{\overline{\overline{\langle h(\tilde{\alpha}_p)\tilde{\alpha}_p(\widetilde{W}_p - \widetilde{W}_g)\rangle}}}$$

The adimensional characteristic length is defined as in the article of Hollloway et al. (2014).

$$\Delta^* = \Delta\ \left(\frac{g}{v_g^2}\right)^{1/3}$$

This parameter presents the advantage to be identical for both types of particles.

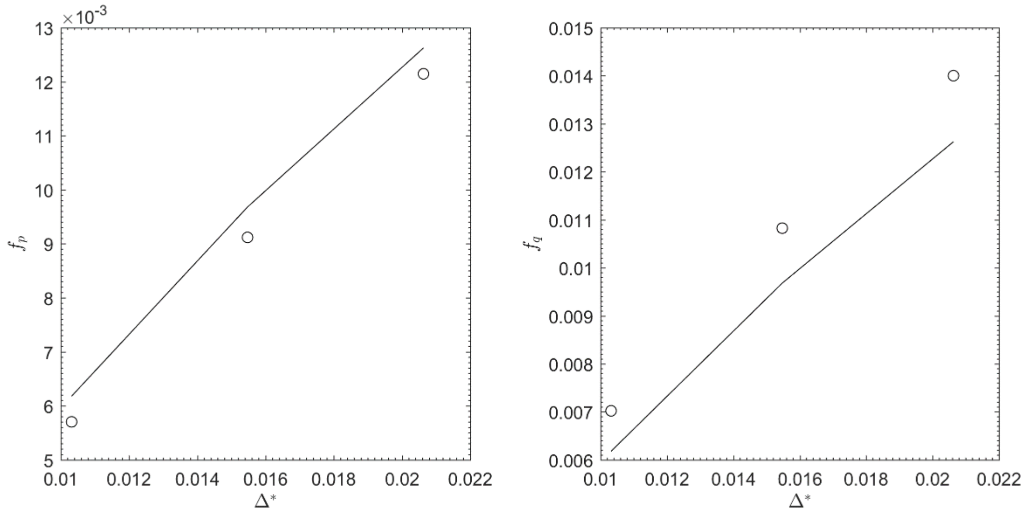

Figure 4 shows the function f for both types of particles.

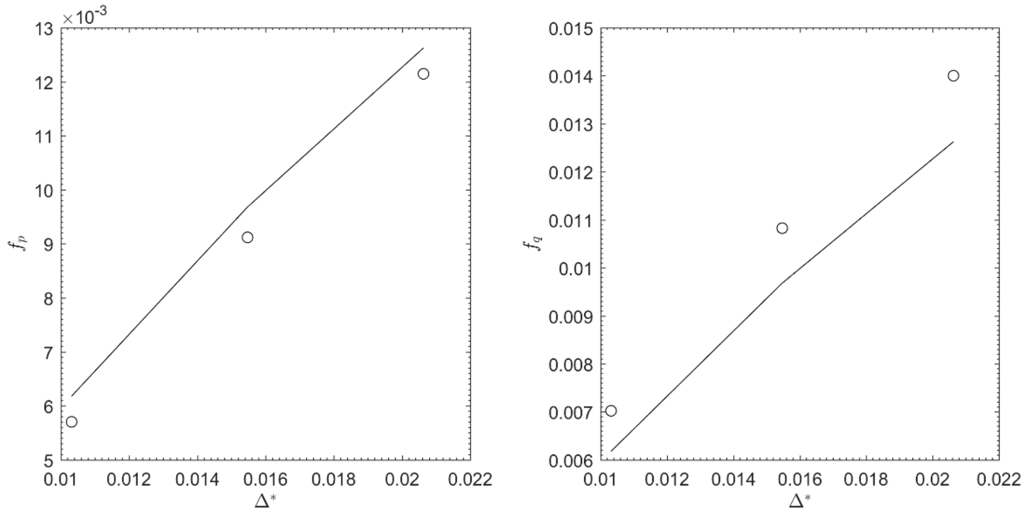

Figure 4: The function f_p for various Δ^*

The function f can be written as a quadratic expression:

$$f(\Delta^*) = C_{f1} + C_{f2}\,\Delta^* + C_{f3}\,{\Delta^*}^2$$

with $C_{f1} = 0,0024$, $C_{f2} = 0{,}95$ and $C_{f3} = 10{,}5$.

3.2 Subgrid inter-particle momentum model

The budget and correlation analysis of the momentum balance equation show that the inter-particle momentum is affected by the mesh. It is in good agreement with the work done by Fede et al. (2013). The correlation analysis suggests that a subgrid inter-particle drift velocity exists and requires a modelling approach. As for the drag force, the inter-particle drift velocity is written in terms of the computed inter-particle relative velocity,

$$\tilde{\alpha}_p \tilde{\alpha}_q W_{pq}^d = \alpha_p \alpha_q \widetilde{\left(W_p - W_q\right)} - \tilde{\alpha}_p \tilde{\alpha}_q (\,\widetilde{W}_p - \widetilde{W}_q)$$

Figure 6 shows the subgrid inter-particle drift flux, $\tilde{\alpha}_p \tilde{\alpha}_q W_{pq}^d$, as a function of the resolved inter-particle drift flux, $\tilde{\alpha}_p \tilde{\alpha}_q (\,\widetilde{W}_p - \widetilde{W}_p)$, for a given filter width.

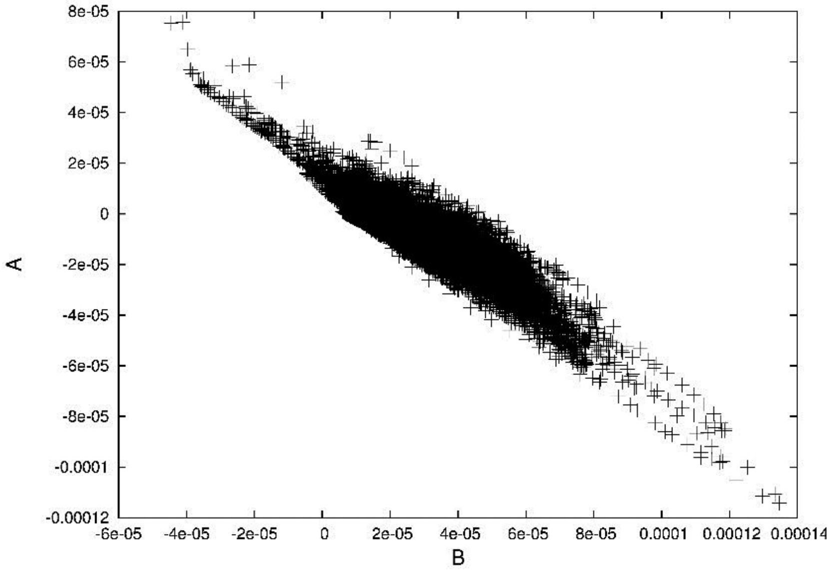

Figure 5: Scatter plot of the subgrid drift flux $A = \tilde{\alpha}_p \tilde{\alpha}_q W^d_{pq}$ versus the resolved drift flux $B = \tilde{\alpha}_p \tilde{\alpha}_q (\widetilde{W}_p - \widetilde{W}_q$ for $\frac{\Delta}{\Delta_{ref}} = 6$

It appears that the two values are correlated. That is why the model proposed is written:

$$\tilde{\alpha}_p \tilde{\alpha}_q W^d_{pq} = g_{pq}\left(\Delta^*_{pq}, \tilde{\alpha}_p, \tilde{\alpha}_q\right) \tilde{\alpha}_p \tilde{\alpha}_q (\widetilde{W}_p - \widetilde{W}_p)$$

The particle volume fractions of the small and large particles appear to be correlated (Figure 6).

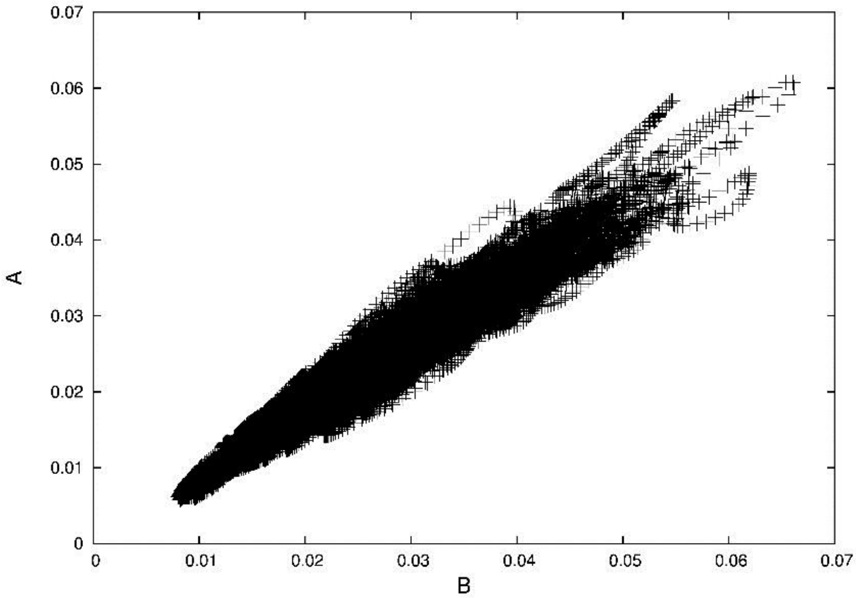

Figure 6: Scatter plot of the solid fraction of particles type q α_q versus the particles volume fraction of the particle type p α_p

Then, instead of using α_p and α_q, the total solid volume fraction α_s is used and the model becomes:

$$\tilde{\alpha}_p \tilde{\alpha}_q W^d_{pq} = g_{pq}\left(\Delta^*_{pq}, \tilde{\alpha}_s\right) \tilde{\alpha}_p \tilde{\alpha}_q (\widetilde{W}_p - \widetilde{W}_q)$$

The model g_{pq} is the inter-particulate correction function that can be calculated:

$$g_{pq}\left(\Delta_{pq}^{*},\tilde{\alpha}_{s}\right)=\frac{\overline{\langle\tilde{\alpha}_{p}\tilde{\alpha}_{q}W_{pq}^{d}|\tilde{\alpha}_{s}\rangle}}{\langle\tilde{\alpha}_{p}\tilde{\alpha}_{q}(\widetilde{W}_{p}-\widetilde{W}_{q})|\tilde{\alpha}_{s}\rangle}$$

The calculated function $g_{pq}\left(\Delta_{pq}^{*},\tilde{\alpha}_{s}\right)$ for different filter widths are shown by Figure 8.

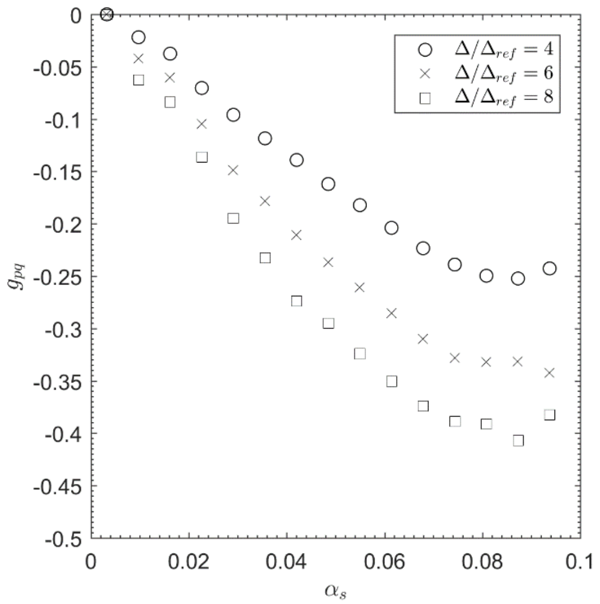

Figure 7: The function g_{pq} for various filter widths

The shape of g_{pq} being almost independent of the filter width, we can decompose $g_{pq}(\Delta^{*},\tilde{\alpha}_{s})$ as:

$$g_{pq}\left(\Delta_{pq}^{*},\tilde{\alpha}_{s}\right)=f_{pq}\left(\Delta_{pq}^{*}\right)h_{pq}(\tilde{\alpha}_{s})$$

As for the drag force, he function g_{pq} is not defined for $\alpha_s > 0.1$. The range of solid volume fraction will be $\alpha_s \in [0;0{,}1]$. The function g_{pq} is normalized by the area under the curve for each filter widths. A form of the function h_{pq} is then proposed.

$$h_{pq}(\tilde{\alpha}_{s})=\left(C_{1}\left(\frac{\tilde{\alpha}_{s}}{\alpha_{max}}\right)^{2}+C_{2}\left(\frac{\tilde{\alpha}_{s}}{\alpha_{max}}\right)+C_{3}\right)\left(\frac{\tilde{\alpha}_{s}}{\alpha_{max}}\right)$$

with $C_1=-6289$, $C_2=834{,}4$ and $C_3=124{,}8$. This function verifies the condition, being equal to 0 when there is no particle.

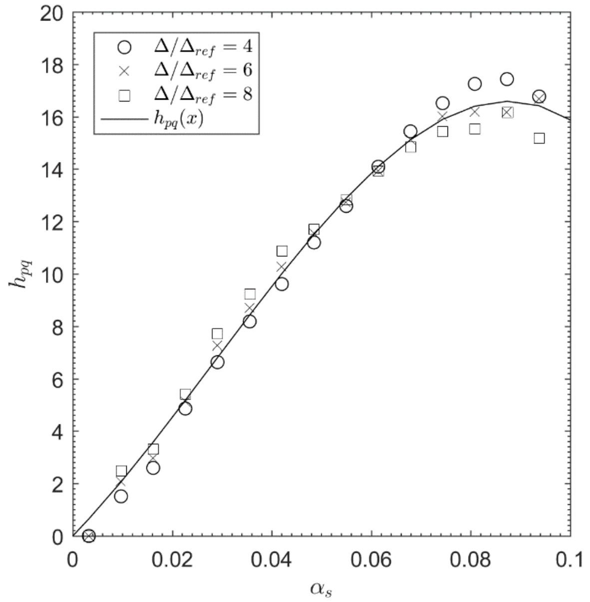

Figure 8: The measured function h_{pq} for various filter widths (symbols) and the proposed correlation (solid lines)

The function $f_{pq}(\Delta^*_{pq})$needs to be defined. The first issue encountered is defining the adimensional characteristic length scale Δ^*_{pq}. Indeed, for the inter-particle momentum transfer, the particle time scale has to be identical of the both particles types. The function f_{pq} ad function of Δ^*_{pq} is shown by Figure 9.

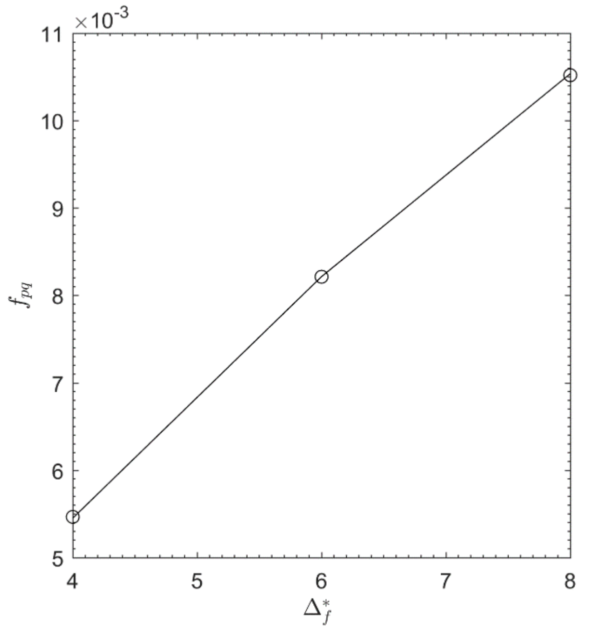

Figure 9: The function f_{pq} for various filter wdiths

The function f_{pq} can be written:

$$f_{pq}(\Delta^*) = P_1 {\Delta^*}^2 + P_2\Delta^* + P_3$$

with $P_1 = -8{,}3, P_2 = 0{,}75$ and $P_3 = \ -0{,}0014$

4 Nomenclature

Symbols

- Δ: characteristic length of cell volume
- Δ_{ref}: characteristic length of cell volume of the refined simulation
- Δ^{*} : adimensional characteristic length scale of cell volume
- $\langle Q \rangle$: a domain averaged of quantity Q
- $\bar{Q}$: a discrete ensemble average value of quantity

Latin symbols

- g_0: radial distribution function
- g_r: mean inter-particle relative velocity
- $H_1(z)$: transition function
- m_g: mass of gas in the computational domain
- m_s: mass of solid in the computational domain
- n_g: mean particle number density
- n_p: mean particle number density
- W_g: mean vertical gas velocity
- W_p: mean vertical particle velocity
- W_{pq}: subgrid relative velocity between particles
- W_{pq}: subgrid relative velocity between particles
- V_{rp}: relative velocity between fluid and particles
- z: parameter quantifying the ratio between the mean inter-particle velocity and the mean relative agitation between the particles species

Greek symbols

- τ_p: particle response time
- ν_g: kinematic gas viscosity
- ρ_g: the gas density
- ρ_p: the p-particle density
- ρ_q the q-particle density
- α_g: gas volume fraction
- α_p: solid volume fraction of p-particles
- α_q: solid volume fraction of q-particles
- $\alpha_s = \alpha_p + \alpha_q$: whole solid volume fraction
- α_{max}: maximum packing

Fede, P.; Ozel, A. & Simonin, O. Effect of unresolved structures on the Euler-Euler simulation of 3D periodic circulating fluidized of binary mixture 8th International Conference on Multiphase Flow, ICMF 2013, Jeju, Korea, May 26 - 31, 2013

Igci, Y.; Andrews IV, A. T.; Sundaresan, S.; Pannala, S. & O'Brien, T. Filtered Two-Fluid Models for Fluidized Gas-Particle Suspensions AIChE Journal, 2008, 54, 1431-1448

Igci, Y. & Sundaresan, S. Verification of filtered two-fluid models for gas-particle flows in risers AIChE Journal, Wiley Subscription Services, Inc., A Wiley Company, 2011, 57, 2691-2707

Holloway, W.; Benyahia, S.; Hrenya, C. M. & Sundaresan, S. Meso-scale structures of bidisperse mixtures of particles fluidized by a gas Chemical Engineering Science , 2011, 66, 4403 – 4420

Holloway, W. & Sundaresan, S. Filtered models for bidisperse gas–particle flows Chemical Engineering Science , 2014, 108, 67 – 86

Milioli, C. C.; Milioli, F. E.; Holloway, W.; Agrawal, K. & Sundaresan, S. Filtered two-fluid models of fluidized gas-particle flows: New constitutive relations AIChE Journal, 2013, 59, 3265-3275

Ozel, A.; Fede, P. & Simonin, O. Development of filtered Euler-Euler two-phase model for circulating fluidised bed: High resolution simulation, formulation and a priori analyses International Journal of Multiphase Flow , 2013, 55, 43-63

Parmentier, J.-F.; Simonin, O. & Delsart, O. A functional subgrid drift velocity model for filtered drag prediction in dense fluidized bed AIChE Journal, Wiley Subscription Services, Inc., A Wiley Company, 2012, 58, 1084-1098

Parmentier, J.-F.; Simonin, O. & Delsart, O. A Numerical Study of Fluidization Behavior of Geldart B, A/B and A Particles Using an Eulerian Multifluid Modeling Approach Proc. of the 9th Int. Conference on Circulating Fluidized Beds, 2008, 331-336